Unraveling Cross-Modality Knowledge Conflicts in Large Vision-Language Models

Anonymous authors
Paper under double-blind review

Abstract

Large Vision-Language Models (LVLMs) have demonstrated impressive capabilities for capturing and reasoning over multimodal inputs. However, these models are prone to parametric knowledge conflicts, which arise from inconsistencies of represented knowledge between their vision and language components. In this paper, we formally define the problem of **cross-modality parametric knowledge conflict** and present a systematic approach to detect, interpret, and mitigate them. We introduce a pipeline that identifies conflicts between visual and textual answers, showing a persistently high conflict rate across modalities in recent LVLMs regardless of the model size. We further investigate how these conflicts interfere with the inference process and propose a contrastive metric to discern the conflicting samples from the others. Building on these insights, we develop a novel dynamic contrastive decoding method that removes undesirable logits inferred from the less confident modality components based on answer confidence. For models that do not provide logits, we also introduce two prompt-based strategies to mitigate the conflicts. Our methods achieve promising improvements in accuracy on both the ViQuAE and InfoSeek datasets. Specifically, using LLaVA-34B, our proposed dynamic contrastive decoding improves an average accuracy of 2.24%.

1 Introduction

Large Vision-Language Models (LVLMs; OpenAI 2023; Anil et al. 2023; Liu et al. 2024) have demonstrated potent capabilities for perceiving and understanding information across different modalities. These models typically consist of a visual encoder and a large language model (LLM), aligned by a projection layer (Li et al., 2022a; Alayrac et al., 2022; Liu et al., 2024). This alignment and collaboration mechanism between the language and vision components allows users to input text and images simultaneously, breeding some of the wildest applications, including retrieving information based on a combination of textual and visual queries (Karthik et al., 2023; Zhang et al., 2024a) and accomplishing complex real-world tasks with multimodal agents (Zhang & Zhang, 2023; Zheng et al., 2024).

However, the disentangled training processes and distinct learning resources leveraged by the vision and language components of an LVLM, respectively, inherently bring along inconsistencies in their learned representations, captured knowledge, as well as their influence during inference (Bartsch et al., 2023; Rabinovich et al., 2023). Given that the visual encoder and the LLM are separately trained on different datasets with distinct training objectives, their parametric knowledge across language and vision modalities is susceptible to conflicts, potentially leading to hallucinations (Ji et al., 2023) and inconsistencies in prediction (Chang & Bergen, 2024). As illustrated in Fig. 1, we present a conflict case from an LVLM. When asked a question about the same entity presented in two different modalities, the LVLM provides two contradictory answers. Even though the visual encoder is able to recognize the `Sydney Opera House` , the model still fails to integrate this information coherently across modalities. This phenomenon reveals a crucial challenge: the disparity between the knowledge captured by the vision and language components of LVLMs. However, there has been limited research on parametric knowledge conflicts within these models, especially concerning cross-modality conflicts. Thus, in this paper, we systematically investigate the phenomenon of

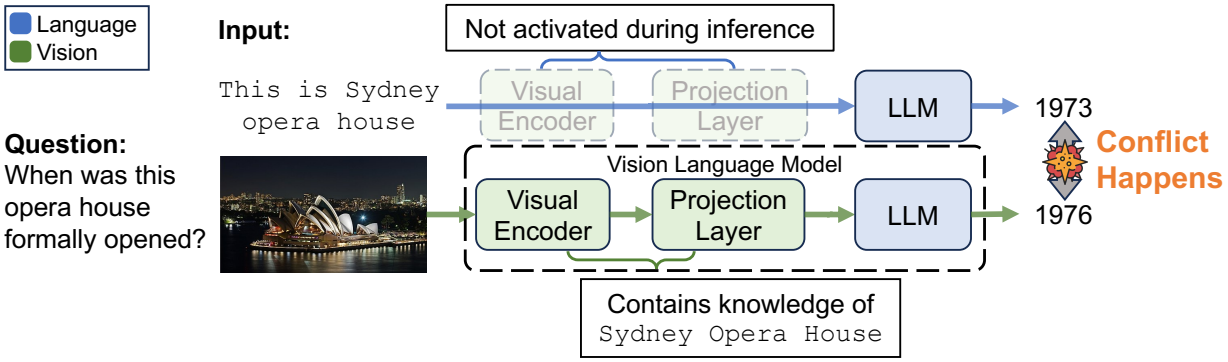

Figure 1: A conflict case of different input modalities with the same information. The conflict still happens even when the visual components recognize the Sydney Opera House.

cross-modality parametric knowledge conflict as defined in §3. We aim to address three principled research questions, as further detailed below:

RQ1: How to detect cross-modality parametric knowledge conflicts? In §4, we introduce a pipeline for detecting such conflicts using a multiple-choice question answering format focused on named entities. Specifically, we present each named entity in different modalities and pose the same question about it. The resulting answers derived from the knowledge of each modality are then compared to determine if a conflict exists. Our findings reveal a persistently high lower bound of the conflict rate across various model scales and architectures, indicating that scaling alone does not resolve these conflicts.

RQ2: How can cross-modality parametric knowledge conflicts be interpreted, especially how they intervene the inference process? Given the severity of knowledge conflicts in LVLMs, this intriguing question arises. One might initially assume that such cross-modal conflicts would reduce the prediction confidence in the original answer due to conflicting parametric knowledge. However, our analyses demonstrate that confidence cannot reliably distinguish between correct and incorrect answers, necessitating a more nuanced interpretation of these conflicts. To address this issue, we propose a contrastive metric in §5 that more effectively identifies conflicting samples. This metric suggests that cross-modality knowledge conflicts actually widen the information gap embedded in the tokens. Moreover, we formulate the metric in an autoregressive form to elicit the memory of visual components and discover a distinct pattern of what different modalities learn.

RQ3: What strategies can be introduced to mitigate cross-modality knowledge conflicts at inference? Having gained an understanding of how these conflicts affect the inference, we seek to address this question. Inspired by the strong discriminatory power of the contrastive metric, we propose a dynamic contrastive decoding method in §6. This method selectively removes undesired logits inferred from the less reliable modality based on answer confidence. Additionally, we propose two prompt-based strategies to mitigate cross-modality knowledge conflicts in cases where the model does not provide logits. Our dynamic contrastive decoding method provides more consistent improvements.

In summary, the main contributions of this paper are threefold: **1)** To the best of our knowledge, this is the first-of-its-kind work to define and study cross-modality parametric knowledge conflicts in LVLMs. **2)** We propose a practical pipeline for detecting such conflicts, along with a metric that distinguishes conflicting samples from non-conflicting ones. **3)** We introduce a dynamic contrastive decoding method to mitigate these conflicts, as well as two prompt-based strategies for closed-source models.

2 Related Work

Knowledge Conflict. Knowledge conflict is a critical problem in context-specific tasks, such as machine reading comprehension (Longpre et al., 2021; Zhou et al., 2023; Wang et al., 2023a) and information extraction (Wang et al., 2022; Fang et al., 2024; Xu et al., 2022; Wang et al., 2023b;c) In the realm of LLMs, recent studies can be categorized into context-memory conflict, inter-context conflict, and intra-memory conflict (Xu et al., 2024). The context-memory conflict and the inter-context conflict are concerned mainly in the process of Retrieval Augmented Generation (RAG). They find that LLMs tend to overly rely on their own parametric memory when facing contradictory evidence (Xie et al., 2023; Wu et al., 2024). The intra-memory

conflict, on the other hand, is rooted in the pre-training corpus, which contains inaccurate and misleading information (Bender et al., 2021; Lin et al., 2021; Kandpal et al., 2023). The inconsistency of knowledge causes LLMs to generate contradictory outputs when given different prompts with the same information (Elazar et al., 2022; Grosse et al., 2023), undermining their reliability. In this context, prior work has not systematically studied this problem for LVLMs, which motivates this work.

Robustness Issues of LVLMs. Although LVLMs have demonstrated significant potential in understanding and reasoning over multimodal inputs, they also face several robustness challenges, including language bias (Niu et al., 2021; Zhang et al., 2024b; Wang et al., 2024a), hallucinations (Huang et al., 2024; Zhu et al., 2024), and the visual perception gap (Ghosh et al., 2024). Language bias refers to the tendency of LVLMs to rely on language patterns learned during LLM pretraining (Niu et al., 2021; Zhang et al., 2024b; Wang et al., 2024a). Hallucinations, which originate from LLMs, pertain to the discrepancies between generated contents and facts from either real-world or user inputs. (Huang et al., 2023; 2024). The visual perception gap refers to the phenomenon that the LVLMs demonstrate proficient knowledge and visual recognition abilities but fail to link their visual recognition to this knowledge (Lee et al., 2023; Ghosh et al., 2024). These issues often overlook the potential conflicts between the visual and textual components of LVLMs, contributing to the aforementioned challenges.

Inference-time Intervention. Inference-time intervention encompasses a range of techniques designed to influence the inference or generation process of LLMs (Damera Venkata & Bhattacharyya, 2022; Li et al., 2024b). These techniques either directly manipulate the logits of the generated tokens or adjust the model parameters during inference. One of the most notable strategies is contrastive decoding (Li et al., 2022b; Leng et al., 2024; Zhang et al., 2024b), which mitigates undesired distributions by removing them from the original distribution. Another approach involves modifying specific layers of LLMs. For instance, ITI (Li et al., 2024b) adjusts model activation during inference by following a set of directions across several attention heads. These methods provide a means for training-free adjustments to LVLMs, significantly reducing the cost compared to readjusting model parameters.

3 Preliminaries

Before diving into parametric knowledge conflicts in LVLMs, we will first outline key definitions and provide an overview of the general experimental setup.

3.1 Definitions

To ground our analysis, we need to define 1) a typical LVLM architecture, and 2) cross-modality parametric knowledge conflicts.

LVLM Architecture. We focus on the general architecture that is adopted by a variety of LVLMs, including LLaVA (Liu et al., 2024), Blip (Li et al., 2023), and Qwen-VL (Bai et al., 2023). Typically, these models consist of a visual encoder V, a projector F, and a language model LM. Given a multimodal input $x_m = \{x_v, x_t\}$, where x_v is the visual input and x_t is the textual input, LVLM first processes x_v with V, resulting in $p_v = V(x_v)$. Then, through the projector F, p_v is projected into the textual embedding space: $e_v = F(p_v)$. Finally, x_t is embedded into the embedding space by the embedding layer of the LM, resulting in $e_t = \text{embed}(x_t)$. The language model then generates the output by the probability $p_{\text{LM}}(y|e_v, e_t)$. So, a contemporary LVLM can be defined as $p_{\text{LM}}(y|F(V(x_v)), \text{embed}(x_t))$.

Cross-Modality Parametric Knowledge Conflict. Since training a large model from scratch is prohibitively costly, LVLMs typically align a vision encoder onto an existing language model. For example, LLaVA (Liu et al., 2024) aligns the pre-trained CLIP visual encoder ViT-L/14 (Radford et al., 2021) with Vicuna (Chiang et al., 2023), which have been separately trained on different data distributions, leading to potential inconsistent parametric knowledge.

To elicit parametric knowledge, we propose to use answers from different modalities as the indicators of the specific parametric knowledge from each modality. Specifically, given a multimodal input $x_m = \{x_v, q\}$, where q is the question regarding the entity in the image x_v, the output y_m is generated by $p_{\text{LM}}(F(V(x_v)), \text{embed}(q)$,

which we define as the *visual answer*. On the contrary, given a textual input $x_t = \{x_e, q\}$, where x_e is the textual description of a named entity and q is the question to the named entity, the output y_t is generated by $p_{\text{LM}}(\text{embed}(x_t))$, which we define as the *textual answer*. Ideally, the textual answer and the visual answer can be viewed as the elicited parametric knowledge from each modality. Thus, if $y_m \neq y_t$, then a parametric knowledge conflict is identified.

3.2 Experimental Setup

3.2.1 Datasets Construction

Original Datasets. Following prior studies on knowledge conflicts(Xie et al., 2023; Wu et al., 2024), we adopt the multiple choice question answering (MCQA) as the form of evaluating cross-modality parametric knowledge conflicts. The rationale for this choice is twofold: manual evaluation of free-form answers is not scalable due to the significant human labor required, while automated evaluation can introduce undesirable model bias. We choose two tasks of knowledge-based visual question answering about named entities:

- ViQuAE (Lerner et al., 2022) is a semi-automatically constructed dataset comprising 3.7K questions about named entities grounded in a visual context, built upon TriviaQA (Joshi et al., 2017). The named entity in the original question is replaced with an image depicting it, requiring the model to answer the question based on the visual context provided.
- InfoSeek (Chen et al., 2023) is a dataset containing 1.3M questions about over 11K visual entities, designed to evaluate the performance of LVLMs in processing visual content while acquiring relevant knowledge. The dataset is automatically constructed from templates of over 300 relations in Wikidata, ensuring a diverse set of questions.

Multiple Choices Construction. Given that the original datasets are free-form question answering, we synthesize distractor choices for each question. These distractor choices must be relevant to the questions to some extent but factually incorrect, to effectively evaluate the model's ability to discern the correct answers. To this end, we employ LLaMA-3-8B (AI@Meta, 2024) to synthesize relevant but incorrect distractor choices. The quality of the generated distractors is discussed in Appx. §A.3.

3.2.2 Evaluation Metrics

We evaluate model performance using two primary metrics: Accuracy and Flip Rate. *Accuracy (Acc)* measures the model's ability to identify the correct answer in the MCQA format. It is calculated as the proportion of questions where the model's predicted answer matches the ground truth:

$$\text{Acc} = \frac{1}{N}\sum_{i=1}^{N} \mathbb{1}(y_i = \hat{y}_i), \tag{1}$$

where N is the number of samples and $\hat{y}_i$ is the gold answer. *Flip Rate (FR)* is defined to quantify the inconsistency of the model's internal knowledge across different modalities. It measures the frequency of conflicting predictions when the model processes visual versus textual inputs for the same question. FR is calculated as:

$$\text{FR} = \frac{1}{N}\sum_{i=1}^{N} \mathbb{1}(y_{v_i} \neq y_{t_i}), \tag{2}$$

where y_{v_i} is the visual answer and y_{t_i} is the textual answer. FR only calculates cases where the textual answer contradicts the visual answer, regardless of the correctness of the answers.

3.2.3 Models

Following prior works on LVLMs (Zhang et al., 2024b; Zhu et al., 2024), we choose the LLaVA series (Li et al., 2024a) for evaluation, as they provide strong performance and a full range of model scales. Moreover, to evaluate how the architecture of LVLMs affects the phenomenon of knowledge conflicts, we adopt InstructBlip (Dai et al., 2023) and Qwen2-VL (Wang et al., 2024b).

4 Detecting Knowledge Conflicts

In this section, we discuss the pipeline to detect parametric knowledge conflicts in LVLMs and evaluate the severity of these conflicts.

4.1 Method

Inputs. As defined in §3.1, the visual answer is generated by asking a question about the entity presented in the image, while the textual answer is induced by replacing the image with the textual description of the named entity. To ensure that equal information is provided across modalities, we design distinct inputs for each, as illustrated in Fig. 1. Specifically, given a multimodal input $x_m = \{x_v, q\} \in \mathcal{D}$, where $\mathcal{D}$ is the dataset, x_v is the image containing the named entity, and q is the question to the named entity in x_v, the visual answer is generated by:

$$y_v \sim p_{\text{VLM}}(x_v, q) = p_{\text{LM}}(F(V(x_v)), \text{embed}(q)). \tag{3}$$

To generate the textual answer, we add an indicator prompt p before the original question, informing the language model about the named entity in the question. p is written as `This is an image of $named_entity`. Thus, the input of the textual answer becomes $x_t = p + q$. The textual answer is then generated by:

$$y_t \sim p_{\text{VLM}}(x_t) = p_{\text{LM}}(\text{embed}(x_t)). \tag{4}$$

Irrelevant Factor Mitigation in Conflict Detection. The visual answers generated from the aforementioned inputs can be regarded as the elicited parametric knowledge from LVLMs. However, these answers are influenced by various other factors. For example, the visual perceiver V might fail to recognize the entity in x_v, resulting in a random guess. These potential issues impede our ability to accurately detect cross-modality parametric knowledge conflicts. To mitigate these factors, we first instruct the LVLM to identify the entity depicted in x_v. If the model output aligns with the ground truth named entity, we assume the knowledge related to the named entity exists in the parametric memory of V and F, implying that any such conflict is not due to a lack of knowledge in V and F.

4.2 Metric

Despite efforts to mitigate the recognition factor in conflict detection, certain factors remain difficult to disentangle. For instance, a model might recognize the entity in x_v, but fail to link it to the parametric knowledge within the LVLMs through the projector F (Ghosh et al., 2024) or falter in its reasoning process. These issues create a *Performance Gap* between the modalities. To isolate and quantify the true knowledge conflict, we estimate both the upper and lower bounds of the conflict rate that is attributed solely to the cross-modality knowledge conflicts. The procedure is as follows:

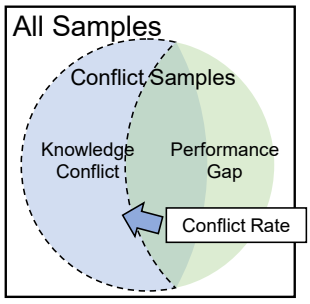

Figure 2: Relationship of conflicting samples.

Determine the upper bound. The FR represents the total proportion of samples where the visual and textual answers differ. This serves as the upper bound for the conflict rate, as it includes conflicts from all sources.

Estimate the performance gap. We estimate the portion of disagreements caused by the Performance Gap. We quantify this gap using the difference in accuracy on correctly recognized entities: $\Delta\text{Acc} = \text{R.Acc}_{\text{textual}} - \text{R.Acc}_{\text{visual}}$. This value represents the percentage of questions the model answers correctly with textual input but fails with visual input, thereby isolating errors introduced specifically by the visual processing pipeline.

Calculate the lower bound. Our core assumption is that the errors captured by ΔAcc are a primary source of the observed flips. To find the conflicts that are not explained by this performance gap, we subtract this value from the total flip rate. This gives us a conservative estimate—a lower bound—for the rate of conflicts that can be attributed purely to inconsistent parametric knowledge.

This relationship is visualized in Fig. 2. The total set of conflicting samples (FR) contains a subset of conflicts that can be explained by the ΔAcc. The remaining samples represent our estimated Conflict Rate

Table 1: Results of detecting cross-modality parametric knowledge conflict. We report accuracy (Acc), recognized accuracy (R. Acc), accuracy difference (ΔAcc), the upper bound of the conflict rate ($FR_{\leq}$) and the lower bound of the conflict rate ($CR_{\geq}$).

Model		ViQuAE					InfoSeek				
		Acc↑	R. Acc↑	ΔAcc↓	$FR_{\leq}$↓	$CR_{\geq}$↓	Acc↑	R. Acc↑	ΔAcc↓	$FR_{\leq}$↓	$CR_{\geq}$↓
LLaVA-7b	Textual	75.65	78.43	20.32	41.68	21.36	52.74	54.55	27.28	70.13	42.85
	Visual	53.26	58.11				22.11	27.27			
LLaVA-13b	Textual	75.65	69.63	8.37	36.47	28.10	56.31	55.41	19.91	58.44	38.53
	Visual	58.57	61.26				31.33	35.50			
LLaVA-34b	Textual	82.46	82.32	4.37	24.90	20.53	66.02	64.07	15.15	43.72	28.57
	Visual	69.14	77.95				44.35	48.92			
InstructBlip-7b	Textual	81.73	80.42	34.79	55.35	20.56	50.53	53.68	15.58	59.74	40.16
	Visual	43.09	45.63				35.17	38.10			
Qwen2-VL-7b	Textual	79.30	78.56	6.19	28.65	22.46	63.24	62.77	2.16	22.51	20.35
	Visual	67.97	72.37				61.69	60.61			

(CR). Therefore, the CR is formulated as:

$$\mathrm{CR} = \frac{N_{kc}}{N} \geq \frac{N_f - N_p}{N} = \mathrm{FR} - \Delta\mathrm{Acc}. \tag{5}$$

In essence, CR filters out the noise from performance errors to provide a clearer signal of the underlying knowledge inconsistency within the model.

4.3 Analysis

We conduct experiments with LVLMs following the aforementioned procedure, and the results are presented in Tab. 1. We report the accuracy (Acc) on the complete evaluation set and the recognized accuracy (R. Acc) on the subset of the evaluation set recognized by the LVLM. Additionally, we calculate the flip rate (FR) and the conflict rate (CR) based on the recognized evaluation set. We also conduct an experiment on free-form generation to prove the generality of cross-modality knowledge conflicts.

Table 2: Results of detecting cross-modality parametric knowledge conflicts in free-form generation.

Model		InfoSeek				
		Acc↑	R. Acc↑	ΔAcc↓	$FR_{\leq}$↓	$CR_{\geq}$↓
Qwen2-VL-7b	Textual	22.51	26.06	2.89	49.07	46.18
	Visual	17.62	23.17			

Performance. For both datasets, the LLaVA-34b model demonstrates the highest accuracy for both textual and visual inputs. However, a significant performance gap exists between the textual and visual answers. The most pronounced performance gap in the LLaVA family is observed in the LLaVA-7b model, where the accuracy difference exceeds 20%. Furthermore, there is a notable improvement in the recognized accuracy (R. Acc) across all models compared to the overall accuracy (Acc). This indicates that the models perform better on recognized entities and that the recognition process effectively mitigates potential factors influencing the final performance.

Conflict Rate. The flip rate (FR) decreases with increasing model size on both datasets, ranging from 55.35% to 24.90% on the ViQuAE dataset. Concurrently, the ΔAcc also declines with larger model sizes, decreasing from 20.32% to 4.37% on the ViQuAE dataset. This trend is more likely to be driven by larger models' improved ability to link visual perception with parametric knowledge and their enhanced reasoning capabilities. When calculating the lower bound of the parametric knowledge conflict rate CR, a consistent pattern emerges across the datasets: LLaVA-7b/13b/34b exhibits values of 21.36%, 28.10%, and 20.53%, respectively. This pattern suggests that regardless of the model's scale and architecture, the likelihood of parametric knowledge conflicts remains relatively constant. For free-form generation, the conflict rate is observed to be higher than in the multiple-choice format. This can likely be attributed to the unconstrained output space, which contributes to an increase of over 25% in both the FR and the CR on Qwen2-VL-7b. To constrain the output space and quantify the results, we will use the MCQA form in the following experiments.

Key Takeaway

There is a clear trend that as the model size increases, both the FR and the ΔAcc between textual and visual answers decrease. However, the lower bound of the knowledge conflict rate (CR) remains consistently high. This suggests that although scaling can enhance the overall performance and consistency, it does not resolve cross-modality knowledge conflicts.

5 Interpreting Knowledge Conflicts

The constantly large conflict rate across datasets highlights the phenomenon caused by cross-modality knowledge conflicts. In this section, we will take a closer look, through the sample-wise perspective, at how parametric knowledge in visual components, *i.e.*, the visual encoder V and the projector F, causes cross-modality parametric knowledge conflict by intervening the inference process of the LLM. In particular, we explore how these conflicts influence answer confidence and propose a metric that can serve as an indicator of the presence of such conflicts.

5.1 Is probability a reliable indicator of answer correctness?

Method. Since the answer probability reflects the model's confidence in a given response, it is natural to consider how parametric knowledge conflicts might affect this probability. For instance, such conflicts may either reduce confidence in the original answer or introduce a more confident alternative answer. Given that embed(x_e) and $F(V(x_v))$ might encapsulate different knowledge, this discrepancy can affect the probability distribution over possible answers, resulting in a shift in confidence in the final output. To investigate how cross-modality parametric knowledge conflict influences answer confidence, we design experiments to determine whether the answer confidence can serve as an indicator of conflict and whether it can suggest the correctness of the answer.

To elicit the answer probability, we calculate the textual answer probability p_t and the visual answer probability p_v using Eq. 3 and Eq. 4. Since we adopt MCQA as the task format, we extract the logits of the answer token, i.e. "A," "B," "C," and "D" and apply the softmax function to them. Thus, the extracted confidence can be presented as $c = \text{softmax}(\log(p[\text{A}]), \log(p[\text{B}]), \log(p[\text{C}]), \log(p[\text{D}]))$, where $p[\text{A}]$ indicates the probability of token "A," and so on. Then, we use the following strategies to understand how visual components influence the inference:

Table 3: Testing different answer correctness indicators based on answer confidence.

Method	ViQuAE	
	Acc	R. Acc
Textual Answer	75.65	78.43
Visual Answer	53.26	58.11
Max Confidence	54.22	60.14
Max Confidence Shift	54.29	60.14
Min Variance Prompt	55.51	61.41
Min Variance Dropout	46.51	50.72

1. *Max confidence*: $\max(c_t[y_t], c_v[y_v])$, where the most confident answer is considered correct.
2. *Max confidence shift*: $\max(c_t[y_t] - c_t[y_v], c_v[y_v] - c_v[y_t])$, where y_t is the textual answer and y_v is the visual answer, indicating that the modality with the most significant influence on the answer is deemed the dominant modality for the question.
3. *Min variance*: $\min(\sigma(c_t[y_t]), \sigma(c_v[y_v]))$, where the answer with the least variance under disturbance is considered the final answer. We introduce disturbance through two methods: writing diverse prompts and applying the Monte Carlo dropout (Gal & Ghahramani, 2016).

Results. The results of three strategies are listed in Tab. 3. From these results, it is evident that none of the strategies based on token probability reliably selects the correct answer when conflicts arise between textual and visual answers. This suggests that: 1) *Confidence is not necessarily reduced by conflicts.* The presence of a cross-modality parametric knowledge conflict does not inherently lower the confidence level of the answer. Instead, the conflict often introduces an alternative answer with higher confidence, overshadowing the original, potentially correct answer. This observation indicates that high confidence alone is not a reliable

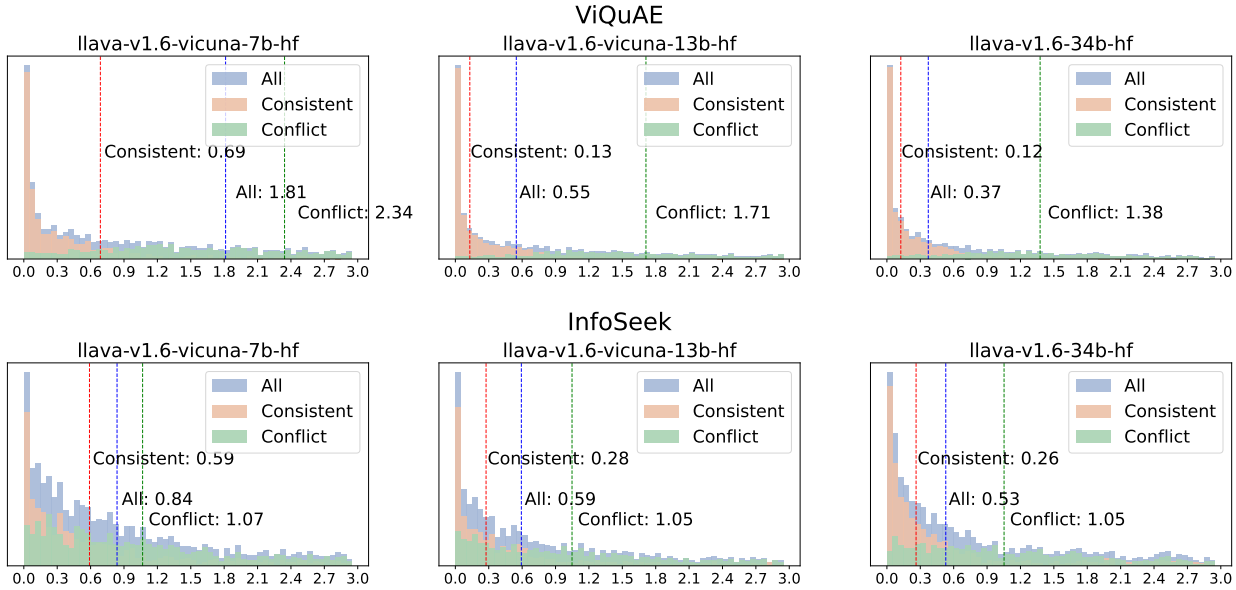

Figure 3: Distribution of the contrastive metric on all samples, samples with modality-consistent answers, and samples with modality-conflict answers. The dashed lines indicate the medians.

indicator of answer correctness in the presence of such conflicts. 2) *Confidence shifts are not indicative of reliability.* The results show that a greater shift in confidence between the textual and visual answers does not necessarily correlate with the reliability of the final answer. 3) *Cross-modality parametric knowledge conflict is not an uncertainty issue.* The table also reveals that methods based on variance do not contribute to the performance. Although these methods attempt to select the more stable answer by selecting the answer with minimum variance in token probability, the results show reductions in accuracy. This implies that minimizing variance does not effectively address the underlying knowledge conflicts.

5.2 Contrastive metric as indicator of conflicts

Method. To effectively understand how conflicting knowledge affects the inference, we utilize the concept of Contrastive Decoding (Li et al., 2022b). Its objective, which subtracts an undesired distribution from the original distribution, serves as a metric for evaluating the degree of divergence between the two distributions. Given that we are using MCQA as the task format, our focus is specifically on the distribution of the answer token, particularly the first token.

Specifically, given a multimodal input $x_m = \{x_v, q\}$, where x_v is the image and q is the question, and a textual input $x_t = \{x_e, q\}$, where x_e is the textual description of the named entity in x_v, the predicted first token distribution of answers for each modality can be represented as Equations (3) and (4). The contrastive objective can then be written as:

$$\log(p_{cd}) = \log(p_v) - \log(p_t) = \log(\frac{p_{\text{VLM}}(y_v|x_v, q)}{p_{\text{VLM}}(y_t|x_e, q)}) = \log(\frac{p_{\text{LM}}(y_v|F(V(x_v)), \text{embed}(q))}{p_{\text{LM}}(y_t|\text{embed}(x_e), \text{embed}(q))}). \tag{6}$$

Ideally, if $F(V(x_v)$ and $\text{embed}(x_e)$ provide the same information for q, Eq. 6 should be equal to 0. However, due to the parametric knowledge conflicts $V(F(x_v))$ may not embed the same knowledge as $\text{embed}(x_e)$, leading to $log(p_{cd}) \not\approx 0$. Thus, $|\log(p_{cd})|$ can be interpreted as the degree of difference between $V(F(x_v))$ and $\text{embed}(x_e)$. Regarding other factors entangled in this difference, the results in §4 have shown that the majority of the inconsistent cases is caused by cross-modality knowledge conflicts. Moreover, the non-random distribution of the contrastive metric also indicates that the inconsistency is not caused by random guessing. Additionally, the contrastive decoding objective also allows us to elicit visual memories by eliminating the influence of textual knowledge.

Result. In Fig. 3, we present the distribution of the contrastive metric, specifically separating samples with consistent answers across modalities from those with conflicting answers. The figure reveals a significant disparity between the consistent and conflicting samples. Most consistent samples fall within the range of

Table 4: Examples of elicited textual and visual memories using the contrastive decoding objective.

Question	Textual Memory	Visual Memory
In what city did Bruce Lee grow up?	San Francisco, California, USA. ✔	Hong Kong. ✗
George Harrison was deported from which city because of his youth?	George Harrison of the Beatles was deported from Hamburg, Germany. ✔	George Harrison was deported from Liverpool, England because of his youth. ✗
What species of fly has the Latin name calliphora vomitoria?	Calliphora vomitoria is a species of fly commonly known as the "fruit fly." ✗	Calliphora vomitoria is commonly known as blue bottle fly. It belongs to family Calliphoridae... ✔
Mary Robinson and Frances Villiers were mistresses of which 19th century King?	King Charles II ✗	Mary Robinson and Frances Villiers were mistresses of King George IV of England. ✔

0-0.6, while conflicting samples exhibit greater variability, with an average median of 1.46. This similar trend suggests that the extent of conflicts is relatively consistent across different models, despite variations in model scales and architectures, implying that the cross-modality parametric knowledge conflicts are not solely dependent on the model's architecture or size but are intrinsic challenges that persist across current training datasets. Moreover, the observed inconsistent generation in LVLMs can also be attributed to conflicts in cross-modality knowledge. This insight reveals a path forward for improving the training of more consistent LVLM models. The figure also suggests that the contrastive metric is effective in distinguishing between consistent and conflicting answers. From the perspective of the contrastive metric, it quantifies the divergence between the knowledge encoded in the visual components and the LLM. Thus, the misaligned knowledge leads to the information gap embedded in the tokens of different modalities, which is ultimately presented by the conflicting answer.

5.3 Eliciting Visual Knowledge

The contrastive decoding objective described in Eq. 6 not only serves as a metric but also offers a valuable tool for examining the memory embedded within the visual components of LVLMs. Specifically, the contrastive decoding metric can be reformulated in an autoregressive form:

$$p_{cd}(y|x) = \prod_{i=1}^{n} p_{cd}(y_i|x, y_{<i}) = \prod_{i=1}^{n} \frac{p_{\text{LM}}(y_v|F(V(x_v)), \text{embed}(q), y_{<i})}{p_{\text{LM}}(y_t|\text{embed}(x_e), \text{embed}(q), y_{<i})}, \tag{7}$$

where x is the inputs from both modalities and $y_{<i}$ indicates the tokens generated before step i. This autoregressive form of contrastive decoding metric allows us to elicit visual memory from the visual components by removing the influence of textual knowledge. We accomplish this by transforming the question into a free-form query without predefined options and then examining the elicited memory of the visual components. The examples of the elicited memories are listed in Tab. 4.

From these memories, several observations can be made:

1. **LLM is better at memorizing date and location.** This aligns intuitively with the nature of the LLM's training process, where such factual knowledge frequently appears in the text corpora. It corresponds well with the expectation that language models acquire structured knowledge from reading-based data.

2. **Visual components are better at memorizing the correlation between an entity and its names and the relationship among entities.** For example, when asked the king of two named mistresses, the language model fails to answer correctly, while the visual memory is correct. This is likely due to the training objective of extending modalities from LLMs (Zhu et al., 2025), aligning visual components with the LLM, during which visual components learn entity-specific knowledge by mapping images to the language space.

Table 5: Results of the dynamic contrastive decoding compared to baselines. **Bold** indicates the bests and underline indicates second bests.

Model	Method	ViQuAE		InfoSeek	
		Acc	R. Acc	Acc	R. Acc
LLaVA-7b	Textual Answer	75.65	78.43	52.74	54.55
	Visual Answer	53.26	58.11	22.11	27.27
	DCD	76.49 (+0.84)	79.51 (+1.08)	54.90 (+2.16)	58.87 (+4.32)
LLaVA-13b	Textual Answer	75.65	69.63	56.31	55.41
	Visual Answer	58.57	61.26	31.33	35.50
	DCD	76.58 (+0.93)	74.14 (+4.51)	58.03 (+1.72)	56.52 (+1.11)
LLaVA-34b	Textual Answer	80.99	82.32	66.02	64.07
	Visual Answer	69.14	77.95	44.35	48.92
	DCD	**83.35** (+2.36)	**85.33** (+3.01)	**68.14** (+2.12)	**67.72** (+3.65)
InstructBlip-7b	Textual Answer	81.73	80.42	50.53	53.68
	Visual Answer	43.09	45.63	35.17	38.10
	DCD	82.47 (+0.74)	80.59 (+0.17)	50.53 (+0.00)	54.38 (+0.70)
Qwen2-VL-7b	Textual Answer	79.30	78.56	63.24	62.77
	Visual Answer	67.97	72.37	61.69	60.61
	DCD	80.76 (+1.46)	80.59 (+2.03)	64.30 (+1.06)	63.34 (+0.57)

Key Takeaway

The proposed contrastive metric effectively distinguishes conflicting samples from consistent ones, suggesting that cross-modality knowledge conflicts tend to exacerbate the information gap between tokens across different modalities , regardless of model scaling or architectural modifications, highlighting the inherent challenge of resolving such conflicts in LVLMs.

6 Mitigating Knowledge Conflicts at Inference Time

Having established an understanding of cross-modality parametric knowledge conflicts, we now shift our focus to strategies for mitigating these conflicts. Since the contrastive metric has proven effective in distinguishing conflicting samples from consistent ones, we first propose a strategy that leverages the principles of contrastive decoding. Moreover, we also design an alternative approach based on prompting for models that do not provide access to logits during inference.

6.1 Dynamic Contrastive Decoding

Method. In an ideal application of contrastive decoding, we would have an a priori knowledge of the logits, which enables us to define the undesired logits. That is to say, to resolve cross-modality parametric knowledge conflicts, the logits from the incorrect, conflicting modality should be excluded from those of the correct modality. However, in real-world scenarios, without external validation, it is impossible to definitively determine the correctness of an answer. Therefore, we propose using the model's answer confidence as a trend for correctness, also treating it as a scaling factor for the original logits. We then apply these scaled logits to the contrastive decoding algorithm, formulating the **dynamic contrastive decoding (DCD)**. This approach adjusts the contrastive decoding objective by incorporating confidence as a dynamic factor to more accurately measure the difference in information embedded by the textual and visual components.

Specifically, given the textual answer y_t with its probabilities $p_t(y_t|x_e, q)$ and the visual answer y_v with its probabilities $p_v(y_v|x_v, q)$, we first calculate the confidence for each answer as follows:

$$c_t = \max(\text{softmax}(\log(p_t[\text{A}]), \log(p_t[\text{B}]), \log(p_t[\text{C}]), \log(p_t[\text{D}]))), \tag{8}$$

$$c_v = \max(\text{softmax}(\log(p_v[\text{A}]), \log(p_v[\text{B}]), \log(p_v[\text{C}]), \log(p_v[\text{D}]))), \tag{9}$$

where p[A] indicates the probability for token "A," and similarly for other tokens. Next, the scaled logits are computed as $s_t = c_t \times \log(p_t)$ and $s_v = c_v \times \log(p_v)$. To assess which modality is more likely to provide the correct answer, we view the confidence as the likelihood, selecting the modality with the higher confidence. However, as discussed in §5.1, confidence alone is insufficient to determine correctness. Therefore, we subtract the scaled logits of the less confident modality from those of the more confident one. This leads to the application of contrastive decoding on the scaled logits, conditioned by the answer confidence:

$$\log(p_{cd}(y|x)) = \begin{cases} c_t \log(p_t) - c_v \log(p_v), \text{if } c_t > c_v \\ c_v \log(p_v) - c_t \log(p_t), \text{otherwise.} \end{cases} \tag{10}$$

Table 6: Experimental results of the InfoSeek dataset on LLaVA-7b and Qwen2-VL-7b.

Model	Method	Acc.	R. Acc.	Model	Method	Acc.	R. Acc.
LLaVA-7b	Textual	52.74	54.55	Qwen2-VL-7b	Textual	63.24	62.77
	Visual	22.11	27.27		Visual	61.69	60.61
	CD	49.05	51.23		*CD*	59.42	60.17
	VCD	23.12	29.34		*VCD*	60.12	61.71
	DCD	**54.90**	**58.87**		***DCD***	**64.30**	**63.34**

Results. Tab. 5 presents the accuracy and the recognized accuracy for different methods across the ViQuAE and InfoSeek datasets. Across both datasets and all model sizes, DCD consistently outperforms both the textual and visual answers. For instance, in the LLaVA-7b model, DCD improves the accuracy from 75.65% to 76.49% on the ViQuAE dataset. Similarly, on the InfoSeek dataset, accuracy increases from 52.74% to 54.90%. These improvements are even more pronounced in the larger models. For example, in the LLaVA-34b model, DCD increases accuracy by 2.36% on the ViQuAE dataset and by 2.12% on InfoSeek, indicating its potential in models with larger scales.

DCD demonstrates particularly significant gains in R. Acc. For instance, on the InfoSeek dataset, the recognized accuracy for the LLaVA-34b model increases by 3.65% when using DCD compared to the textual answer. This trend is consistent across all model sizes, indicating that DCD is particularly effective in improving the performance on recognized entities. The improvement in recognized accuracy is likely due to the fact that the visual answers within the recognized set are expected to contain more relevant information than those in the unrecognized set, as the visual components have some prior knowledge of these entities. Consequently, the DCD can more effectively leverage this information to discern which option is correct. ~~For the ablation study, we also compare DCD with contrastive decoding in Appx. §C.~~ Tab. 6 shows the comparison between the naive contrastive decoding (CD) and the visual contrastive decoding (VCD). The results indicate that DCD outperforms other contrastive decoding based methods, proving the effectivness of DCD on mitigating cross-modality knowledge conflicts.

6.2 Prompting Strategy

Method. Since not all models provide the logits of the generated contents, we propose two prompt-based improvement strategies for those models.

1. *Reminder prompt.* Once a knowledge conflict is detected , the model is prompted to regenerate the answer with a reminder that highlights the potential presence of conflicting knowledge. This prompt require the model to decide internally which modality is more reliable.

2. *Answer prompt.* Since both textual and visual answers are already generated during the detection process, this prompt asks the model to determine which is correct.

Results. Tab. 7 presents the results of prompt-based improvements using two strategies across two datasets and different model sizes. The effectiveness of these strategies depends on the model size. For smaller models, both prompts negatively impact performance across both datasets, with accuracy dropping by at least 1.07% on the ViQuAE dataset and 0.86% on the InfoSeek dataset. This suggests that smaller models may struggle to handle prompts reminding them of potential knowledge conflicts. Furthermore, presenting smaller models with conflicting answers seems to introduce additional confusion, evidenced by the more substantial accuracy

Table 7: Results of the prompt-based strategies compared to the baselines. Since the inputs of this experiment are the same as generating visual answers, we compare them to the results of the visual answer. **Bold** indicates best results and underline indicates second bests.

Method	ViQuAE		InfoSeek	
	Acc	R. Acc	Acc	R. Acc
LLaVA-7b				
Visual Answer	53.26	58.11	22.11	27.27
Reminder Prompt	53.99 (-1.66)	57.25 (-2.53)	21.25(-0.86)	27.99 (+0.72)
Answer Conflict Prompt	54.58 (-1.07)	58.51 (-1.27)	20.23 (-1.88)	27.39 (+0.12)
LLaVA-13b				
Visual Answer	58.57	61.26	31.33	35.50
Reminder Prompt	58.57 (+0.00)	61.26 (+0.00)	35.53 (+4.20)	38.10 (+2.60)
Answer Conflict Prompt	57.59 (-0.98)	59.67 (-1.59)	34.27 (+2.94)	39.06 (+3.56)
LLaVA-34b				
Visual Answer	69.14	77.95	44.35	48.92
Reminder Prompt	72.99 (+3.85)	79.28 (+1.33)	45.15 (+0.80)	49.62 (+0.70)
Answer Conflict Prompt	**73.62** (+4.48)	**79.66** (+1.71)	**52.43** (+8.08)	**53.68** (+4.76)

declines. In contrast, larger models leverage the prompts effectively, achieving accuracy gains of 4.48% and 8.08% on ViQuAE and InfoSeek, respectively. These findings suggest that prompt-based conflict strategy becomes more effective with model scale, particularly when both conflicting answers are provided.

Key Takeaway

Dynamic contrastive decoding (DCD) brings universal improvements against the baselines. When the visual components recognize the entity, the logits contain more information than those that are not recognized. The performance of prompting-based strategies varies depending on the model size. Larger models are better at understanding and processing the designed instructions.

7 Conclusions

In this paper, we introduce the concept of cross-modality parametric knowledge conflicts in LVLMs, stemming from misalignments between visual and textual modalities. We propose a systematic approach to detect these conflicts, revealing a persistently high conflict rate across all model sizes and showing that scaling alone does not resolve these issues. Building on this, we propose the contrastive metric, which effectively identifies conflicting samples by measuring the information gap between modalities. Further, we introduce dynamic contrastive decoding (DCD), which selectively removes unreliable logits to improve answer accuracy. For models without access to logits, we propose two prompt-based strategies. These approaches collectively improve model performance. On LLaVA-34B, DCD achieves an accuracy improvement of 2.36% on the ViQuAE dataset and 2.12% on the InfoSeek dataset. Our study advances the understanding of cross-modality parametric knowledge conflicts in LVLMs and provide practical solutions to mitigate them, leading to more robust multimodal inference.

References

AI@Meta. Llama 3 model card, 2024. URL `https://github.com/meta-llama/llama3/blob/main/MODEL_CARD.md`.

Jean-Baptiste Alayrac, Jeff Donahue, Pauline Luc, Antoine Miech, Iain Barr, Yana Hasson, Karel Lenc, Arthur Mensch, Katherine Millican, Malcolm Reynolds, et al. Flamingo: a visual language model for few-shot learning. *Advances in neural information processing systems*, 35:23716–23736, 2022.

Rohan Anil, Andrew M Dai, Orhan Firat, Melvin Johnson, Dmitry Lepikhin, Alexandre Passos, Siamak Shakeri, Emanuel Taropa, Paige Bailey, Zhifeng Chen, et al. Palm 2 technical report. *arXiv preprint arXiv:2305.10403*, 2023.

Jinze Bai, Shuai Bai, Shusheng Yang, Shijie Wang, Sinan Tan, Peng Wang, Junyang Lin, Chang Zhou, and Jingren Zhou. Qwen-vl: A versatile vision-language model for understanding, localization, text reading, and beyond, 2023.

Henning Bartsch, Ole Jorgensen, Domenic Rosati, Jason Hoelscher-Obermaier, and Jacob Pfau. Self-consistency of large language models under ambiguity. *arXiv preprint arXiv:2310.13439*, 2023.

Emily M Bender, Timnit Gebru, Angelina McMillan-Major, and Shmargaret Shmitchell. On the dangers of stochastic parrots: Can language models be too big? In *Proceedings of the 2021 ACM conference on fairness, accountability, and transparency*, pp. 610–623, 2021.

Tyler A Chang and Benjamin K Bergen. Language model behavior: A comprehensive survey. *Computational Linguistics*, 50(1):293–350, 2024.

Yang Chen, Hexiang Hu, Yi Luan, Haitian Sun, Soravit Changpinyo, Alan Ritter, and Ming-Wei Chang. Can pre-trained vision and language models answer visual information-seeking questions? *arXiv preprint arXiv:2302.11713*, 2023.

Wei-Lin Chiang, Zhuohan Li, Zi Lin, Ying Sheng, Zhanghao Wu, Hao Zhang, Lianmin Zheng, Siyuan Zhuang, Yonghao Zhuang, Joseph E. Gonzalez, Ion Stoica, and Eric P. Xing. Vicuna: An open-source chatbot impressing gpt-4 with 90%* chatgpt quality, March 2023. URL `https://lmsys.org/blog/2023-03-30-vicuna/`.

Wenliang Dai, Junnan Li, Dongxu Li, Anthony Meng Huat Tiong, Junqi Zhao, Weisheng Wang, Boyang Li, Pascale Fung, and Steven Hoi. Instructblip: Towards general-purpose vision-language models with instruction tuning. *arXiv preprint arXiv:2308.01525*, 2023.

Niranjan Damera Venkata and Chiranjib Bhattacharyya. When to intervene: Learning optimal intervention policies for critical events. *Advances in Neural Information Processing Systems*, 35:30114–30126, 2022.

Yanai Elazar, Nora Kassner, Shauli Ravfogel, Amir Feder, Abhilasha Ravichander, Marius Mosbach, Yonatan Belinkov, Hinrich Schütze, and Yoav Goldberg. Measuring causal effects of data statistics on language model'sfactual'predictions. *arXiv preprint arXiv:2207.14251*, 2022.

Tianqing Fang, Zhaowei Wang, Wenxuan Zhou, Hongming Zhang, Yangqiu Song, and Muhao Chen. Getting sick after seeing a doctor? diagnosing and mitigating knowledge conflicts in event temporal reasoning. In Kevin Duh, Helena Gomez, and Steven Bethard (eds.), *Findings of the Association for Computational Linguistics: NAACL 2024*, pp. 3846–3868, Mexico City, Mexico, June 2024. Association for Computational Linguistics. doi: 10.18653/v1/2024.findings-naacl.244. URL `https://aclanthology.org/2024.findings-naacl.244`.

Yarin Gal and Zoubin Ghahramani. Dropout as a bayesian approximation: Representing model uncertainty in deep learning. In *international conference on machine learning*, pp. 1050–1059. PMLR, 2016.

Sreyan Ghosh, Chandra Kiran Reddy Evuru, Sonal Kumar, Utkarsh Tyagi, Oriol Nieto, Zeyu Jin, and Dinesh Manocha. Vdgd: Mitigating lvlm hallucinations in cognitive prompts by bridging the visual perception gap, 2024.

Roger Grosse, Juhan Bae, Cem Anil, Nelson Elhage, Alex Tamkin, Amirhossein Tajdini, Benoit Steiner, Dustin Li, Esin Durmus, Ethan Perez, et al. Studying large language model generalization with influence functions. *arXiv preprint arXiv:2308.03296*, 2023.

Lei Huang, Weijiang Yu, Weitao Ma, Weihong Zhong, Zhangyin Feng, Haotian Wang, Qianglong Chen, Weihua Peng, Xiaocheng Feng, Bing Qin, et al. A survey on hallucination in large language models: Principles, taxonomy, challenges, and open questions. *arXiv preprint arXiv:2311.05232*, 2023.

Wen Huang, Hongbin Liu, Minxin Guo, and Neil Zhenqiang Gong. Visual hallucinations of multi-modal large language models. *arXiv preprint arXiv:2402.14683*, 2024.

Ziwei Ji, Nayeon Lee, Rita Frieske, Tiezheng Yu, Dan Su, Yan Xu, Etsuko Ishii, Ye Jin Bang, Andrea Madotto, and Pascale Fung. Survey of hallucination in natural language generation. *ACM Computing Surveys*, 55(12):1–38, 2023.

Mandar Joshi, Eunsol Choi, Daniel S Weld, and Luke Zettlemoyer. Triviaqa: A large scale distantly supervised challenge dataset for reading comprehension. *arXiv preprint arXiv:1705.03551*, 2017.

Nikhil Kandpal, Haikang Deng, Adam Roberts, Eric Wallace, and Colin Raffel. Large language models struggle to learn long-tail knowledge. In *International Conference on Machine Learning*, pp. 15696–15707. PMLR, 2023.

Shyamgopal Karthik, Karsten Roth, Massimiliano Mancini, and Zeynep Akata. Vision-by-language for training-free compositional image retrieval. *arXiv preprint arXiv:2310.09291*, 2023.

Jiyoung Lee, Seungho Kim, Seunghyun Won, Joonseok Lee, Marzyeh Ghassemi, James Thorne, Jaeseok Choi, O-Kil Kwon, and Edward Choi. Visalign: Dataset for measuring the degree of alignment between ai and humans in visual perception. *arXiv preprint arXiv:2308.01525*, 2023.

Sicong Leng, Hang Zhang, Guanzheng Chen, Xin Li, Shijian Lu, Chunyan Miao, and Lidong Bing. Mitigating object hallucinations in large vision-language models through visual contrastive decoding. In *Proceedings of the IEEE/CVF Conference on Computer Vision and Pattern Recognition*, pp. 13872–13882, 2024.

Paul Lerner, Olivier Ferret, Camille Guinaudeau, Hervé Le Borgne, Romaric Besançon, José G Moreno, and Jesús Lovón Melgarejo. Viquae, a dataset for knowledge-based visual question answering about named entities. In *Proceedings of the 45th International ACM SIGIR Conference on Research and Development in Information Retrieval*, pp. 3108–3120, 2022.

Bo Li, Kaichen Zhang, Hao Zhang, Dong Guo, Renrui Zhang, Feng Li, Yuanhan Zhang, Ziwei Liu, and Chunyuan Li. Llava-next: Stronger llms supercharge multimodal capabilities in the wild, May 2024a. URL `https://llava-vl.github.io/blog/2024-05-10-llava-next-stronger-llms/`.

Junnan Li, Dongxu Li, Caiming Xiong, and Steven Hoi. Blip: Bootstrapping language-image pre-training for unified vision-language understanding and generation. In *International conference on machine learning*, pp. 12888–12900. PMLR, 2022a.

Junnan Li, Dongxu Li, Silvio Savarese, and Steven Hoi. Blip-2: Bootstrapping language-image pre-training with frozen image encoders and large language models. In *International conference on machine learning*, pp. 19730–19742. PMLR, 2023.

Kenneth Li, Oam Patel, Fernanda Viégas, Hanspeter Pfister, and Martin Wattenberg. Inference-time intervention: Eliciting truthful answers from a language model. *Advances in Neural Information Processing Systems*, 36, 2024b.

Xiang Lisa Li, Ari Holtzman, Daniel Fried, Percy Liang, Jason Eisner, Tatsunori Hashimoto, Luke Zettlemoyer, and Mike Lewis. Contrastive decoding: Open-ended text generation as optimization. *arXiv preprint arXiv:2210.15097*, 2022b.

Stephanie Lin, Jacob Hilton, and Owain Evans. Truthfulqa: Measuring how models mimic human falsehoods. *arXiv preprint arXiv:2109.07958*, 2021.

Haotian Liu, Chunyuan Li, Qingyang Wu, and Yong Jae Lee. Visual instruction tuning. *Advances in neural information processing systems*, 36, 2024.

Shayne Longpre, Kartik Perisetla, Anthony Chen, Nikhil Ramesh, Chris DuBois, and Sameer Singh. Entity-based knowledge conflicts in question answering. In Marie-Francine Moens, Xuanjing Huang, Lucia Specia, and Scott Wen-tau Yih (eds.), *Proceedings of the 2021 Conference on Empirical Methods in*

Natural Language Processing, pp. 7052–7063, Online and Punta Cana, Dominican Republic, November 2021. Association for Computational Linguistics. doi: 10.18653/v1/2021.emnlp-main.565. URL https://aclanthology.org/2021.emnlp-main.565.

Yulei Niu, Kaihua Tang, Hanwang Zhang, Zhiwu Lu, Xian-Sheng Hua, and Ji-Rong Wen. Counterfactual vqa: A cause-effect look at language bias. In *Proceedings of the IEEE/CVF conference on computer vision and pattern recognition*, pp. 12700–12710, 2021.

OpenAI. Gpt-4 technical report. *arXiv preprint arXiv:2303.08774*, 2023.

Ella Rabinovich, Samuel Ackerman, Orna Raz, Eitan Farchi, and Ateret Anaby-Tavor. Predicting question-answering performance of large language models through semantic consistency. *arXiv preprint arXiv:2311.01152*, 2023.

Alec Radford, Jong Wook Kim, Chris Hallacy, Aditya Ramesh, Gabriel Goh, Sandhini Agarwal, Girish Sastry, Amanda Askell, Pamela Mishkin, Jack Clark, Gretchen Krueger, and Ilya Sutskever. Learning transferable visual models from natural language supervision, 2021.

Fei Wang, Wenjie Mo, Yiwei Wang, Wenxuan Zhou, and Muhao Chen. A causal view of entity bias in (large) language models. In Houda Bouamor, Juan Pino, and Kalika Bali (eds.), *Findings of the Association for Computational Linguistics: EMNLP 2023*, pp. 15173–15184, Singapore, December 2023a. Association for Computational Linguistics. doi: 10.18653/v1/2023.findings-emnlp.1013. URL https://aclanthology.org/2023.findings-emnlp.1013.

Fei Wang, Wenxuan Zhou, James Y Huang, Nan Xu, Sheng Zhang, Hoifung Poon, and Muhao Chen. mdpo: Conditional preference optimization for multimodal large language models. In *EMNLP*, 2024a.

Haoyu Wang, Hongming Zhang, Yuqian Deng, Jacob Gardner, Dan Roth, and Muhao Chen. Extracting or guessing? improving faithfulness of event temporal relation extraction. In Andreas Vlachos and Isabelle Augenstein (eds.), *Proceedings of the 17th Conference of the European Chapter of the Association for Computational Linguistics*, pp. 541–553, Dubrovnik, Croatia, May 2023b. Association for Computational Linguistics. doi: 10.18653/v1/2023.eacl-main.39. URL https://aclanthology.org/2023.eacl-main.39.

Peng Wang, Shuai Bai, Sinan Tan, Shijie Wang, Zhihao Fan, Jinze Bai, Keqin Chen, Xuejing Liu, Jialin Wang, Wenbin Ge, et al. Qwen2-vl: Enhancing vision-language model's perception of the world at any resolution. *arXiv preprint arXiv:2409.12191*, 2024b.

Yiwei Wang, Muhao Chen, Wenxuan Zhou, Yujun Cai, Yuxuan Liang, Dayiheng Liu, Baosong Yang, Juncheng Liu, and Bryan Hooi. Should we rely on entity mentions for relation extraction? debiasing relation extraction with counterfactual analysis. In Marine Carpuat, Marie-Catherine de Marneffe, and Ivan Vladimir Meza Ruiz (eds.), *Proceedings of the 2022 Conference of the North American Chapter of the Association for Computational Linguistics: Human Language Technologies*, pp. 3071–3081, Seattle, United States, July 2022. Association for Computational Linguistics. doi: 10.18653/v1/2022.naacl-main.224. URL https://aclanthology.org/2022.naacl-main.224.

Yiwei Wang, Bryan Hooi, Fei Wang, Yujun Cai, Yuxuan Liang, Wenxuan Zhou, Jing Tang, Manjuan Duan, and Muhao Chen. How fragile is relation extraction under entity replacements? In *Proceedings of the 27th Conference on Computational Natural Language Learning (CoNLL)*, pp. 414–423, 2023c.

Siye Wu, Jian Xie, Jiangjie Chen, Tinghui Zhu, Kai Zhang, and Yanghua Xiao. How easily do irrelevant inputs skew the responses of large language models? *arXiv preprint arXiv:2404.03302*, 2024.

Jian Xie, Kai Zhang, Jiangjie Chen, Renze Lou, and Yu Su. Adaptive chameleon or stubborn sloth: Revealing the behavior of large language models in knowledge conflicts. *arXiv preprint arXiv:2305.13300*, 2023.

Nan Xu, Fei Wang, Bangzheng Li, Mingtao Dong, and Muhao Chen. Does your model classify entities reasonably? diagnosing and mitigating spurious correlations in entity typing. In Yoav Goldberg, Zornitsa Kozareva, and Yue Zhang (eds.), *Proceedings of the 2022 Conference on Empirical Methods in Natural*

Language Processing, pp. 8642–8658, Abu Dhabi, United Arab Emirates, December 2022. Association for Computational Linguistics. doi: 10.18653/v1/2022.emnlp-main.592. URL https://aclanthology.org/2022.emnlp-main.592.

Rongwu Xu, Zehan Qi, Cunxiang Wang, Hongru Wang, Yue Zhang, and Wei Xu. Knowledge conflicts for llms: A survey. *arXiv preprint arXiv:2403.08319*, 2024.

Kai Zhang, Yi Luan, Hexiang Hu, Kenton Lee, Siyuan Qiao, Wenhu Chen, Yu Su, and Ming-Wei Chang. Magiclens: Self-supervised image retrieval with open-ended instructions. *arXiv preprint arXiv:2403.19651*, 2024a.

Yi-Fan Zhang, Weichen Yu, Qingsong Wen, Xue Wang, Zhang Zhang, Liang Wang, Rong Jin, and Tieniu Tan. Debiasing large visual language models. *arXiv preprint arXiv:2403.05262*, 2024b.

Zhuosheng Zhang and Aston Zhang. You only look at screens: Multimodal chain-of-action agents. *arXiv preprint arXiv:2309.11436*, 2023.

Boyuan Zheng, Boyu Gou, Jihyung Kil, Huan Sun, and Yu Su. Gpt-4v (ision) is a generalist web agent, if grounded. *arXiv preprint arXiv:2401.01614*, 2024.

Wenxuan Zhou, Sheng Zhang, Hoifung Poon, and Muhao Chen. Context-faithful prompting for large language models. In Houda Bouamor, Juan Pino, and Kalika Bali (eds.), *Findings of the Association for Computational Linguistics: EMNLP 2023*, pp. 14544–14556, Singapore, December 2023. Association for Computational Linguistics. doi: 10.18653/v1/2023.findings-emnlp.968. URL https://aclanthology.org/2023.findings-emnlp.968.

Lanyun Zhu, Deyi Ji, Tianrun Chen, Peng Xu, Jieping Ye, and Jun Liu. Ibd: Alleviating hallucinations in large vision-language models via image-biased decoding. *arXiv preprint arXiv:2402.18476*, 2024.

Tinghui Zhu, Kai Zhang, Muhao Chen, and Yu Su. Is extending modality the right path towards omni-modality? *arXiv preprint arXiv:2506.01872*, 2025.

Table 8: Distractor Example

Question: Which protected area is this building usually located in?
Choices: ['The Peak District', 'Yorkshire Dales', 'North York Moors', 'Lake District']

A Experimental Details

A.1 Experimental Setup

Confidence Analysis. We will describe the experimental setup of the *Min variance* strategy in §5.1. For both settings, we sample 10 times with disturbance. For the prompt disturbance, we ask the LLaMA-3-8b (AI@Meta, 2024) to rephrase the original prompt to obtain 10 different prompts and generate the answer with each of them. For the dropout disturbance, we set the dropout rate to 0.1 and sample 10 times. Then we extract the confidence of the gold answer and calculate the variance.

A.2 Prompts

The details of the prompts used in our experiments are listed here. The prompt to generate false options is in Tab. 11. The reminder prompt to mitigate knowledge conflicts is in Tab. 12. The answer conflict prompt to mitigate knowledge conflicts is in Tab. 13.

A.3 Distractor Quality

The quality of our generated distractors is manually evaluated to ensure they are both correctly formatted and contextually relevant. An example of a question with its corresponding correct answer and generated distractors is shown in Tab. 8. We randomly sample 200 samples from the InfoSeek dataset and assess the generated distractors against two primary criteria:

1. **Format Consistency:** The distractors must match the data type and format of the correct answer. For example, if the correct answer is a specific date like "July 26, 1990," a generated distractor such as "in 1990" would be considered a format violation.

2. **Semantic Relevance:** The distractors must belong to the same semantic category as the correct answer. In the example shown in Tab. 8, the correct answer, "Lake District," is a national park. All generated distractors are also well-known national parks in the UK, making them highly plausible but incorrect choices. A distractor like "London" would be a relevance violation, as it is a city, not a protected area.

Our manual evaluation revealed a high level of quality. Out of the 200 samples, only 3 violated the format consistency criterion, and a mere 2 violated the semantic relevance criterion. These results confirm that our generation method produces high-quality and challenging distractors suitable for our evaluation framework.

B Case Study

Tab. 9 presents several conflicting cases that reveal a clear division of labor between modalities. The visual modality excels at recognizing visual features, such as colors, as seen in the correct identification of the Paphiopedilum acmodontum. In contrast, the textual modality is more effective at recalling factual information, including dates and names, as demonstrated by the correct prediction of the language of the Trojan War story. This functional specialization aligns with the dual nature of human learning, which integrates knowledge from both visual perception and textual sources.

C ~~Ablation Study~~

Table 9: Case study of conflicting cases in the recognized set of the ViQuAE.

Question	Choices	Textual Answer	Visual Answer
What is the common name for calliphora vomitoria?	A: Housefly; B: Flesh Fly; C: Bluebottle; D: Blow Fly	A ✗	C ✓
What color spots do Paphiopedilum acmodontum have?	A: Black; B: Brown; C: White; D: Red	A ✗	B ✓
What language was the story where Cebriones and his half-brother Hector fight using chariots in the Trojan War written in?	A: Latin; B: German; C: Italian; D: Greek	D ✓	A ✗
What year was the team that played Arsenal in the 1969 Football League Cup Final founded?	A: 1791; B: 1879; C: 1867; D: 1932	B ✓	C ✗

~~We conduct experiments on the LLaVA-7b model to compare the proposed DCD and the traditional contrastive decoding method, where the latter omits the confidence scaling in Eq. 10. The results, presented in Tab. 10, indicate that the confidence scaling is effective in resolving cross-modality knowledge conflicts, which further suggests that the answer confidence encapsulates valuable information about the relative informativeness of each modality for a given question. While confidence alone may not serve as a reliable indicator, the rich information it conveys can be leveraged to enhance overall performance.~~

Table 10: Experimental results of the overall accuracy on the ViQuAE and the InfoSeek dataset.

	ViQuAE	InfoSeek
CD	70.10	49.05
DCD	76.49	54.90

Table 11: Prompt for generating false options to construct the multiple-choice question answering datasets.

Given the question and its gold answer, please generate a multiple choice version of this question. Note that the wrong choices should be relevant to the question and the gold answer should be exactly copied from what is given. You can randomly put the gold answer wherever you want. Please output as a json format: {"A": Answer A, "B": Answer B, "C": Answer C, "D": Answer D}. No further explanation or note.

Table 12: Reminder prompt to mitigate cross-modality parametric knowledge conflicts.

You are an expert at question answering. Given the question, please output the answer. No explanation and further question. Be aware that your visual memory might differ from your textual memory, causing a conflict in your knowledge.

Table 13: Answer conflict prompt to mitigate cross-modality parametric knowledge conflicts.

You are an expert at question answering. Given the question, please output the answer. No explanation and further question. Be aware that your visual memory might differ from your text memory, causing a conflict in your knowledge. Your text memory is: {textual answer} and your visual memory is: {visual answer}.